International Journal of Modern Physics B, Vol. 12, Nos. 27 & 28 (1998) 2831–2845

MEAN-FIELD ANALYSIS OF THE THREE-BAND HUBBARD MODEL

YABIN YU*,†,‡, GUANGHAN CAO† and ZHENGKUAN JIAO†
†*Department of Physics, Zhejiang University, Hangzhou 310027, PR China*
‡*Department of Physics, Yantai University, Yantai 264005, PR China*

Received 18 May 1998

A full three-band model for the CuO_2 plane of cuprates, which includes all the essential interaction — Cu-O and O-O hopping and the Coulomb repulsion on the Cu and O sites and between them, is considered. Its antiferromagnetic ground state for the half-filling is studied by using the mean field approximation. The electronic structure and the magnetic properties such as the densities of states, the energy spectra, the composition of holes (Cu or O character), the superexchange interaction and the magnetic moment are calculated and in general, our results are in agreement with the available experimental and other calculation results. Meanwhile, we find that the influence of the O-O hopping and Cu-O intrasite Coulomb repulsion on these properties is considerable. Our estimate of the energy of the spin singlet state above the antiferromagnetic background indicates that the lowest excitation state of the holes is the singlet state and give a charge-transfer energy in agreement with the experiment. We also discuss the hole-doping to the antiferromagnetic background and find the mean field approach invalid. Finally, based on the electronic structure at the half-filling, en effective one-band Hubbard model is presented and the effective parameters are close to the values given by the computation on the clusters.

1. Introduction

Since the discovery of the high-T_c superconducting cuprates, the two-dimensional (2D) electronic system with strong correlation has been extensively studied in order to understand the specialty of electronic properties in the cuprate superconductors. Several theoretical models for the system were proposed, such as the one-band Hubbard model,[1] three-band Hubbard,[2] the t–J model,[3] the three-band t–J model[4] and the p–d model.[5] The three-band Hubbard model is commonly believed to provide a suitable starting point in the description of the CuO_2 planes in the cuprates. In fact, both the relevant features of the systems, the strong local repulsion on copper and the strong p–d hybridization between oxygen and copper, are contained in this model. Zhang and Rice,[3] starting from the three-band Hubbard model derived a one-band effective Hamiltonian that is the t–J model. This model has been widely adopted to study various electronic properties of the cuprates and succeeded to certain extent.[6] But Emery and Reiter[7] argued that the resulting quasiparticles of

*To whom all the correspondence should be addressed.

the three-band model have both charge and spin, in contrast to the Cu-O singlets that form the effective one-band t–J model. Zhang and Rice[8] and Emery and Reiter[9] continued their exchange of idea on this subject. On the other hand, Chen, Schutter and Fedro,[10] Schutter and Fedro[11] and Hybertsen *et al.*[12] have presented fairly convincing evidence which indicates that the reduction to a one-band model is possible. Other authors[13,14] have also contributed to the discussion. Recently, spin-resolved photoemmision[15] shows that the top of the valance band in CuO is of pure singlet character, which provides strong support for the existence of Zhang and Rice singlet in the high-T_c cuprate superconductors.

The purpose of our paper is to give a description of electronic properties for the ground state of three-band Hubbard model at half-filling using the mean-field approximation and present a reduction of the electronic structure for the doped cuprate superconductors. As mentioned above, a great deal of work,[2–14,16–21] has been carried out in studying the three-band model and its reduction to a one-band model. In the most of them, the numerical calculations were performed in a finite lattice using computational techniques, or pretreatments to the model were carried out. The mean field approach is self-consistent, but it is difficult to judge how close to the actual properties of the model its results are. However, as well known, Hartree–Fock approximation can give good description for a half-filled system in the strong coupling limit and the cuprates has been proved to be right in the strong-coupling regime.[6] Using the mean field approximation, Oles and Zaanen[20] analytically studies three-band model in strong coupling limit and gave an numerical results of one-dimensional model for intermediate coupling that they thought to be relevant to the high-T_c superconductors. But they neglected the O-O hopping and the repulsion on oxygen and between copper and oxygen, while the O-O hopping and the repulsion between copper and oxygen have been found to have considerable effect on the properties of the system.[4,16,21] Caprara and Grilli[4] studied the three-band t–J model using a similar approach.

Here, we will give a mean field analysis of the electronic structure and magnetic properties by using Hartree–Fock (HF) approximation for the full two-dimensional three-band Hubbard model which includes all the essential interactions, i.e., Cu-O and O-O hopping and the Coulomb repulsion on copper and oxygen and between them. The parameters of the model are taken the values listed in Ref. 6, which have been widely adopted. In the case of half-filling, we give an antiferromagnetic (AFM) ground state (or near ground state) — a spin density wave (SDW) state. The electronic properties such as the magnetic moment, the superexchange and the antiferromagnetic gap are calculated and the results are in good agreement with the available experimental and other calculation results. The dependence of the parameters of the model on our results is also investigated and we find that the effect of the O-O hopping and Cu-O intrasite Coulomb repulsion on these properties is remarkable. Our result shows that the contribution from O-O hopping t_{pp} to J is about 2/3 of the total value, which is in accordance with the exact cluster calculations made by Eskes and Jefferson.[21] Using the results of Zhang and Rice[3] and Belinicher and Chernyshev,[14] we calculate the energy of a spin singlet in

the AFM background state and show that the first excitation state of holes is this singlet state and then give the correct charge-transfer gap (≈ 2.5 eV). The hole-doping into the AFM background is discussed, yet it is proved that the correct results can not be obtained in the mean field picture. Finally, following from the electronic structure at the half-filling, we present an effective one-band Hubbard model.

2. Model and Formula

The Hamiltonian of the three-band Hubbard model studied here is

$$\begin{aligned} H = & \frac{1}{2}\sum_{i\delta\sigma}\varepsilon_p n^p_{i+\delta\sigma} + \sum_{i\delta\sigma} t_{pd} P_\delta (d^+_{i\sigma} c_{i+\delta\sigma} + \text{H.c.}) \\ & + \sum_{i\delta\delta'} t_{pp} P_{\delta-\delta'} (c^+_{i+\delta} c_{i+\delta'} + \text{H.c.}) + \frac{U_d}{2}\sum_{i\sigma} n^d_{i\sigma} n^d_{i-\sigma} \\ & + \frac{U_p}{2}\sum n^p_{i\sigma} n^p_{i-\sigma} + V\sum_{i\delta} n^d_i n^p_{i+\delta}\,, \end{aligned} \tag{1}$$

where $d^+_{i\delta}$ creates a $d_{x^2-y^2}$ hole with spin σ at a Cu site and $c^+_{i+\delta\sigma}$ creates a p_x or p_y hole with spin σ at a nearest O site of Cu (at ith site). The p-d hybridization between d-hole and p-hole is given by t_{pd} and t_{pp} is the O-O hopping. Due to the p and d symmetry of the Cu and O orbits (Fig. 1), the phase factors in Eq. (1) are $P_\delta = -1$ if $\delta = (1/2, 0)$ or $\delta = (0, -1/2)$ and $P_\delta = 1$ if $\delta = (-1/2, 0)$ or $\delta = (0, 1/2)$; and $P_{\delta-\delta'} = -1$ if $\delta - \delta' = (\pm 1/2, \pm 1/2)$ and $P_{\delta-\delta'} = 1$ if $\delta - \delta' = (\pm 1/2, \mp 1/2)$. U_d and U_p are the onsite repulsion on the Cu and O sites and V is the Cu-O intersite repulsion. Initially we set $U_p = 0$ and $V = 0$.

Performing a mean-field treatment to the Hamiltonian according to HF approximation and selecting the AFM state, we arrive at the following HF Hamiltonian

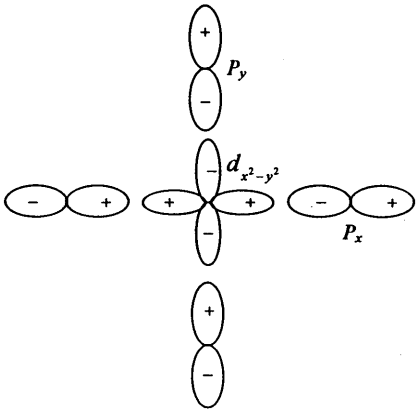

Fig. 1. Scheme of the orbitals included in the three-band model and the phase convention.

$$H = \frac{1}{2}\sum_{i\delta\sigma}\varepsilon_p n^p_{i+\delta\sigma} + \sum_{i\delta\sigma} t_{pd}P_\delta(d^+_{i\sigma}c_{i+\delta\sigma} + \text{H.c.})$$
$$+ \sum_{i\delta\delta'} t_{pp}P_{\delta-\delta'}(c^+_{i+\delta}c_{i+\delta'} + \text{H.c.}) + \frac{U_d}{2}\sum_{i\sigma}(\langle n_d\rangle - S_{i\sigma})n^d_{i\sigma}$$
$$- U_d\sum_{i\sigma}\langle n^d_{i-\sigma}\rangle\langle n^d_{i\sigma}\rangle\,, \tag{2}$$

with

$$S_{i\sigma} = S_\sigma e^{i\mathbf{Q}\cdot\mathbf{R}_i}\,,$$

where $\langle\cdots\rangle$ is the mean value in the ground state, and $\langle n_d\rangle = \langle n^d_{i\uparrow}\rangle + \langle n^d_{i\downarrow}\rangle$; the wave vector $\mathbf{Q} = (\pi,\pi)$ corresponds to the two sublattice AF structure; $S_\sigma = \langle n^d_{i\sigma}\rangle - \langle n^d_{i-\sigma}\rangle$, where i belong to the up-moment sublattice.

Transforming $d_{i\sigma}$ and $c_{i\sigma}$ into momentum space by using

$$c_{\alpha i\sigma} = \frac{1}{\sqrt{N}}\sum_{\mathbf{k}} c_{\alpha\mathbf{k}\sigma}e^{i\mathbf{k}\cdot(\mathbf{R}+\delta)}\,, \tag{3}$$

$$d_{i\sigma} = \frac{1}{\sqrt{N}}\sum_{\mathbf{k}} d_{\mathbf{k}\sigma}e^{i\mathbf{k}\cdot\mathbf{R}_i}\,, \tag{4}$$

where α is x or y depending on $\delta = (\pm 1/2, 0)$ or $\delta = (0, \pm 1/2)$ and then performing transformations $c_{x\mathbf{k}\sigma} \to ic_{x\mathbf{k}\sigma}$ and $c_{y\mathbf{k}\sigma} \to -ic_{y\mathbf{k}\sigma}$, we obtain the following Hamiltonian

$$H = \sum_{\alpha\mathbf{k}\sigma}\varepsilon_p(c^+_{\alpha\mathbf{k}\sigma}c_{\alpha\mathbf{k}\sigma} + c^+_{\alpha\mathbf{k}+Q\sigma}c_{\alpha\mathbf{k}+Q\sigma})$$
$$+\frac{U_d\langle n_d\rangle}{2}\sum_{\mathbf{k}\sigma}(d^+_{\mathbf{k}\sigma}d_{\mathbf{k}\sigma} + d^+_{\mathbf{k}+Q\sigma}d_{\mathbf{k}-Q\sigma})$$
$$- t_{pp}\sum_{\alpha\neq\beta\mathbf{k}\sigma}\{s_{\alpha\mathbf{k}}s_{\beta\mathbf{k}}c^+_{\alpha\mathbf{k}\sigma}c_{\beta\mathbf{k}\sigma} + s_{\alpha\mathbf{k}+Q}s_{\beta\mathbf{k}+Q}c^+_{\alpha\mathbf{k}+Q\sigma}c_{\beta\mathbf{k}+Q\sigma}\}$$
$$-\frac{U_d}{2}\sum_{\mathbf{k}\sigma}S_\sigma(d^+_{\mathbf{k}\sigma}d_{\mathbf{k}+Q\sigma} + \text{H.c.})$$
$$+ t_{pd}\sum_{\alpha\mathbf{k}\sigma}\{s_{\alpha\mathbf{k}}d^+_{\mathbf{k}\sigma}c_{\alpha\mathbf{k}\sigma} + s_{\alpha\mathbf{k}+Q}d^+_{\mathbf{k}+Q\sigma}c_{\alpha\mathbf{k}-Q\sigma}\} + \text{H.c.}\} \tag{5}$$

with

$$s_{\alpha\mathbf{k}} = 2\sin(\mathbf{k}_\alpha/2)\,, \tag{6}$$

here $\mathbf{k}$ is restricted to the magnetic Brilluin zone, i.e., one-half of the first Brillouin zone. For simplicity the last term of Eq. (3) is dropped. We can write the Hamiltonian (6) in the form of matrix as the following

$$H = \sum_{\mathbf{k}\sigma} H_{\mathbf{k}\sigma}\,, \tag{7}$$

where

$$H_{\mathbf{k}\sigma} = \begin{bmatrix} \varepsilon_p & -t_{pp}s_{x\mathbf{k}}s_{y\mathbf{k}} & t_{pd}s_{x\mathbf{k}} & 0 & 0 & 0 \\ -t_{pp}s_{x\mathbf{k}}s_{y\mathbf{k}} & \varepsilon_p & t_{pd}s_{y\mathbf{k}} & 0 & 0 & 0 \\ t_{pd}s_{x\mathbf{k}} & t_{pd}s_{y\mathbf{k}} & U_d n_d/2 & 0 & 0 & -U_d S_\sigma/2 \\ 0 & 0 & 0 & \varepsilon_p & -t_{pp}s_{x\mathbf{k}+Q}s_{y\mathbf{k}+Q} & t_{pd}s_{x\mathbf{k}+Q} \\ 0 & 0 & 0 & -t_{pp}s_{x\mathbf{k}+Q}s_{y\mathbf{k}+Q} & \varepsilon_p & t_{pd}s_{x\mathbf{k}+Q} \\ 0 & 0 & -U_d S_\sigma/2 & t_{pd}s_{x\mathbf{k}+Q} & t_{pd}s_{y\mathbf{k}+Q} & U_d n_d/2 \end{bmatrix}.$$

By introducing the Green's function

$$G_{\mathbf{k}\sigma}(E) = [E - H_{\mathbf{k}\sigma}]^{-1}, \tag{8}$$

we can obtain several Green's functions $G^{ab}_{\mathbf{k}\sigma}(E), G^{ab}_{\mathbf{k}+Q\sigma}(E)$ and $G^{ab}_{\mathbf{k},\mathbf{k}+Q\sigma}(E)$, where a, b indicate the p and d states. Consequently, the self-consistent equations for mean-field parameters n_d and S are given by

$$\begin{aligned} n_d &= -\frac{2}{N\pi}\int_{-\infty}^{\mu} dE \sum_{\mathbf{k}} \mathrm{Im}\{G^{dd}_{\mathbf{k}\sigma}(E+i0^+) + G^{dd}_{\mathbf{k}\sigma}(E+i0^+)\}, \\ S &= -\frac{4}{N\pi}\int_{-\infty}^{\mu} dE \sum_{\mathbf{k}} \mathrm{Im}\{G^{dd}_{\mathbf{k},\mathbf{k}+Q\uparrow}(E+i0^+)\}, \\ n &= \langle n_p\rangle + \langle n_d\rangle = -\frac{2}{N\pi}\int_{-\infty}^{\mu} dE \sum_{\mathbf{k}} \mathrm{Im}\{\mathrm{Tr}\ G_{\mathbf{k}\sigma}(E+i0^+)\}, \end{aligned} \tag{9}$$

where $S = |S_\sigma|$ is the size of the magnetic moment and $\langle n_p\rangle = \langle n^p_\uparrow\rangle + \langle n^p_\downarrow\rangle$; μ is the chemical potential of the holes. In the case of half-filling (i.e. $n = 1$), Eq. (9) becomes

$$\begin{aligned} S &= -\frac{4}{N\pi}\sum_{\mathbf{k}} A^{dd}_{\mathbf{k},\mathbf{k}+Q\uparrow}(E^1_{\mathbf{k}}), \\ n_d &= -\frac{2}{N\pi}\sum_{\mathbf{k}} \{A^{dd}_{\mathbf{k}\sigma}(E^1_{\mathbf{k}}) + A^{dd}_{\mathbf{k}+Q\sigma}(E^1_{\mathbf{k}}), \end{aligned} \tag{10}$$

here $A^{ab}_{\mathbf{k}}(E)$ is defined as $\mathrm{Im}\ G^{ab}_{\mathbf{k}\sigma}(E+i0^+) = A^{ab}_{\mathbf{k}\sigma}(E)\sum_l \delta(E - E^l_{\mathbf{k}})$ and $E^l_{\mathbf{k}}$ is lth pole of $G^{ab}_{\mathbf{k}\sigma}(E)$ (i.e. the eigenenergy of Hamiltonian (7)) and $E^l_{\mathbf{k}}$ is the lowest one. The total energy of the holes per unit cell in the CuO_2 plane can be given by

$$E_{\mathrm{T}} = -\frac{2}{N\pi}\int_{-\infty}^{\mu} EdE \sum_{\mathbf{k}} \mathrm{Im}\{\mathrm{Tr}\ G_{\mathbf{k}\sigma}(E)\} - \frac{1}{4}U_d(n_d + S)(n_d - S). \tag{11}$$

For the ferromagnetic (FM) state, the HF Hamiltonian is reduced to

$$H = \sum_{\alpha\mathbf{k}\sigma} \varepsilon_p C^+_{\alpha\mathbf{k}\sigma} c_{\alpha\mathbf{k}\sigma} + \frac{U_d}{2} \sum_{\mathbf{k}\sigma} (\langle n_d \rangle - S_\sigma) d^+_{\mathbf{k}\sigma} d_{\mathbf{k}\sigma} - t_{pp} \sum_{\alpha\beta\mathbf{k}\sigma} s_{\alpha\mathbf{k}} s_{\beta\mathbf{k}} c^+_{\alpha\mathbf{k}\sigma} c_{\beta\mathbf{k}\sigma} + t_{pd} \sum_{\alpha\mathbf{k}\sigma} s_{\alpha\mathbf{k}} d^+_{\mathbf{k}\sigma} c_{\alpha\mathbf{k}\sigma} + \text{H.c.}\} \,, \tag{12}$$

and Eq. (7) is reduced to a 3×3 matrix.

When the U_p and V are taken into account, HF Hamiltonian and the total energy E_T can be corrected by

$$\varepsilon_p \to \varepsilon_{p\sigma} = \varepsilon_p + 2Vn_d + \frac{1}{2} U_p \langle n^p_{-\sigma} \rangle \,, \qquad \varepsilon_d = 2V \langle n_p \rangle \,, \tag{13}$$

and

$$\Delta E_\text{T} = -\frac{1}{2} U_p \langle n^p_\uparrow \rangle \langle n^p_\downarrow \rangle - 2V \langle n_d \rangle \langle n_p \rangle \,. \tag{14}$$

3. Numerical Results and Discussion

3.1. *Case of the half-filling*

First, we discuss the electronic structure and the magnetic properties of the system described by Eq. (1) at half-filling. We will concentrate mainly on the set of parameters that has been widely accepted. These parameters are $U_d = 10.5$ eV, $t_{pp} = 1.3$ eV, $t_{pp} = 0.65$ eV, $\varepsilon_p = 3.6$ eV, $U_p = 4.0$ eV and $V = 1.2$ eV. Meanwhile, the dependence of the electronic properties on the parameters will be also discussed.

In Fig. 2, we present the electronic structure of the AFM state at the half-filling for the three-band model, where the hole notation is used. Figure 2(a) shows the densities of sates (DOS) $\rho(E)$ calculated by

$$\rho(E) = -\frac{2}{N\pi} \sum_{\mathbf{k}} \text{Tr}\{\text{Im}\, G_{\mathbf{k}\sigma}(E + i\varepsilon)\} \,, \tag{15}$$

where we take $\varepsilon = 0.02$ eV. There are three main parts in the DOS, the lowest and uppermost ones are the lower- and upper-Hubbard bands which are dominated by Copper holes and between them are the oxygen-dominant bands. The energy spectra are presented in Fig. 2(b), in which there are six branches of the energy spectra $E^l_\mathbf{k}$. Through carefully analysis, we know that the six branch of energy spectra correspond to the bonding lower-Hubbard (BLH) band (curve a), the bonding upper-Hubbard band (BUH) band (curve b), the antibonding lowerer-Hubbard band (curve c), the nonbonding bands (curves d and e) and the antibonding upper-Bubbard band (curve f). The two lowest bands are the BLH and BUH bands, so the doping (of hole or electron) is only related to these two bands.

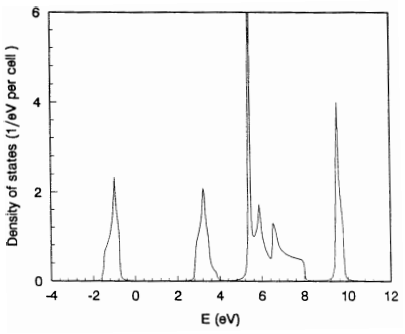

(a)

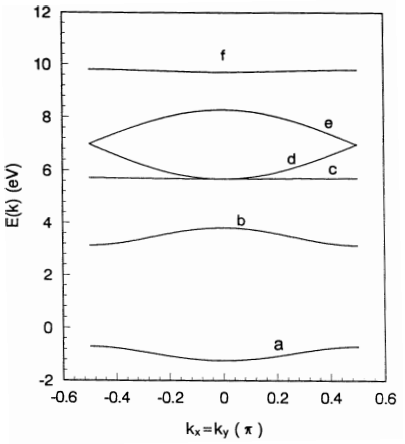

(b)

Fig. 2. (a) Density of states of the three-band model in the AFM state. Here the hole notation is used. Parameters: $\varepsilon_p = 3.6$ eV, $t_{pd} = 1.3$ eV, $t_{pp} = 0.65$ eV, $U_d = 10.5$ eV, $U_p = 4$ eV and $V = 1.2$ eV. (b) Energy spectra of holes. Curves a, b, c, d–e and f correspond to bonding lower Hubbard (BLH), bonding upper Hubbard (BUH), antibonding lower Hubbard, nonbonding and antibonding upper Hubbard bands respectively. The parameters are taken as (a).

In Fig. 3, we present the energy difference between the FM and AFM states as a function of ε_p. This energy difference, in fact, is the superexchange interaction J. We can compare the dependence of J upon ε_p and t_{pp} (Fig. 3(a)) with that of Eskes and Jefferson,[21] and find fairly good agreement except for the case of $t_{pp} = -0.65$ in which our result is similar to that of them for the Cu_2O_7 cluster. Taking $\varepsilon_p = 3.6$ eV and $t_{pp} = 0.65$ eV, we can obtain $J \approx 0.12$ eV and this value is in very good agreement with the experimental results.[22] As illustrated in Ref. 21, the contribution of t_{pp} to J is quite large. When $t_{pp} = 0$ and other parameters are taken as above, $J \approx 0.044$ eV is only about 1/3 of the total value of J. So, about 2/3 of the superexchange interaction is caused by channels involving t_{pp}. This result

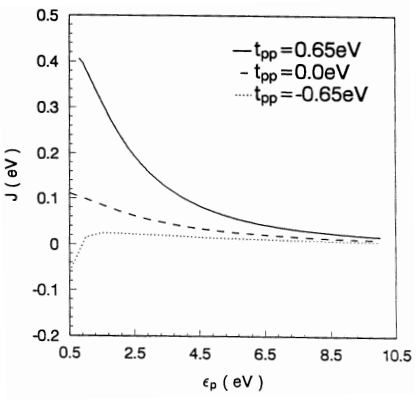

(a)

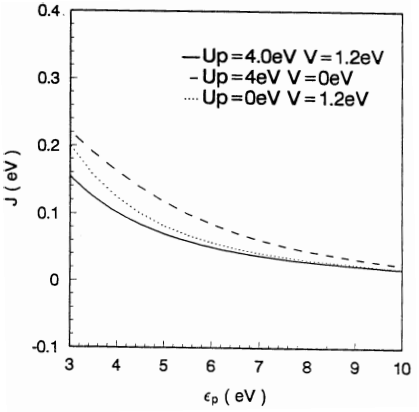

(b)

Fig. 3. Superexchange interaction constant J as a function of ε_p. (a) The solid, dashed and dotted lines correspond to $t_{pp} = 0.65$ eV, $t_{pp} = 0$ eV and $t_{pp} = -0.65$ eV respectively. Other parameters: $t_{pd} = 1.3$ eV, $U_d = 10.5$ eV, $U_p = 4$ eV and $V = 1.2$ eV. (b) Curves for the variation of U_p and V. The solid line stands for $U_p = 4$ eV and $V = 1.2$ eV; the dashed line for $U_p = 4$ eV and $V = 0$ eV; the dotted line for $U_p = 0$ eV and $V = 1.2$ eV. Other parameters are taken as (a).

is in accordance with the result obtained by Eskes and Jefferson.[21] From Fig. 3(b), one can find that the effect of the intrasite repulsion V on J is larger than that of onsite O repulsion U_p in the realistic region of ε_p (around 3.6 eV) and for a larger ε_p the effect of V is still remarkable, while that of U_p may be neglected.

The results for magnetic moment S and hole densities $\langle n_d \rangle$ and $\langle n_p \rangle$ are presented in Figs. 4 and 5. When $\varepsilon_p = 3.6$ eV and $t_{pp} = 0.65$ eV, we can obtain $\langle n_d \rangle \approx 0.77$ and $\langle n_p \rangle \approx 0.23$, roughly being in agreement with the experimental[23] and computational results[12] (i.e., $\langle n_d \rangle = 0.8$ and $\langle n_p \rangle = 0.2$). However, the value of moment $S \approx 0.75$, which is larger, compared with the experimental results

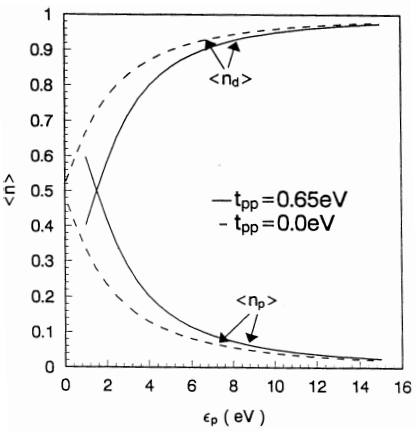

(a)

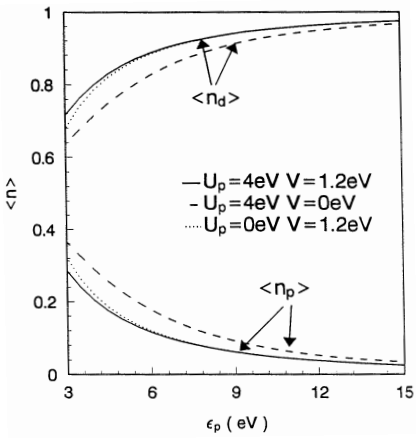

(b)

Fig. 4. Hole density $\langle n_d \rangle$ and $\langle n_p \rangle$ in the AFM state. (a) Solid line, $t_{pp} = 0.65$ eV; dashed line, $t_{pp} = 0$ eV. The top curves correspond to $\langle n_d \rangle$, and the bottom curves correspond to $\langle n_p \rangle$. Parameters: $t_{pd} = 1.3$ eV, $U_d = 10.5$ eV, $U_p = 4$ eV and $V = 1.2$ eV. (b) Curves for the variation of U_p and V. The solid line stands for $U_p = 4$ eV and $V = 1.2$ eV; the dashed line for $U_p = 4$ eV and $V = 0$ eV; the dotted line for $U_p = 0$ eV and $V = 1.2$ eV. Other parameters are taken as (a).

(= 0.4–0.66).[24,25] In the mean field treatment, the quantum spin fluctuation (QSF) has been neglected, but the suppression of QSF to the magnetic moment is very important. For instance, in the two-dimensional, $s = 1/2$ Heiseberg model the magnetic moment is reduced to 0.36–0.38. Using the Random phase approximation in the SDW background, Schrieffer *et al.*[26] investigated the suppression of QSF to the magnetic moment in the one-band Hubbard model and showed that for the strong onsite Coulomb interaction the reduction of the moment is serious. From the above results, one can find that the system is indeed in the localized region

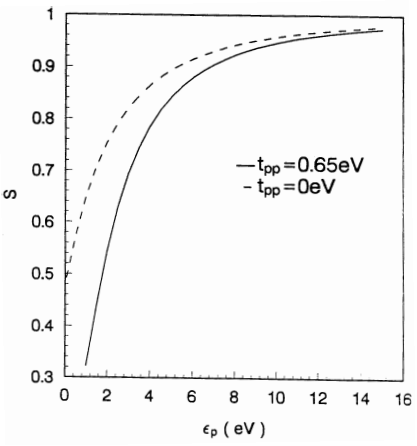

(a)

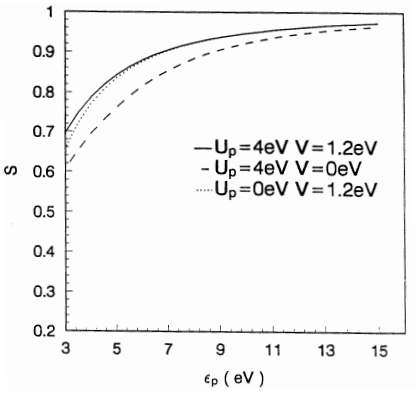

Fig. 5. Magnetic moment S per Cu site. (a) Solid line, $t_{pp} = 0.65$ eV, dashed line, $t_{pp} = 0$ eV. Parameters: $t_{pd} = 1.3$ eV, $U_d = 10.5$ eV, $U_p = 4$ eV and $V = 1.2$ eV. (b) The curves for the variation of U_p and V. The solid line stands for $U_p = 4$ eV and $V = 1.2$ eV; the dashed line for $U_p = 4$ eV and $V = 0$ eV; the dotted line for $U_p = 0$ eV and $V = 1.2$ eV. Other parameters taken as (a).

and nearly no double-occupied on the d-orbits, so our mean filed approximation is reasonable. In Figs. 4 and 5, we also present the dependence of t_{pp}, U_p and V on the results, which indicates that the effect of t_{pp} and V is stronger than that of U_p in the realistic region of ε_p.

In Fig. 6, we present the result for AF gap $E_{\rm gap}$, i.e., the energy gap between the BUH band and BLH band. The gap increases with the increasing value of ε_p, both for $t_{pp} = 0$ eV and $t_{pp} = 0.65$ eV. But, for a given value of ε_p, $E_{\rm gap}(t_{pp} = 0) > E_{\rm gap}(t_{pp} \neq 0)$. It can be seen that for larger ε_p, the energy gap tend to U_d, which corresponds to the complete Mott-insulator. For a small $\varepsilon_p(> 0)$, when the t_{pp} is considered, the gap disappears at a finite value of ε_p; when the t_{pp} is not

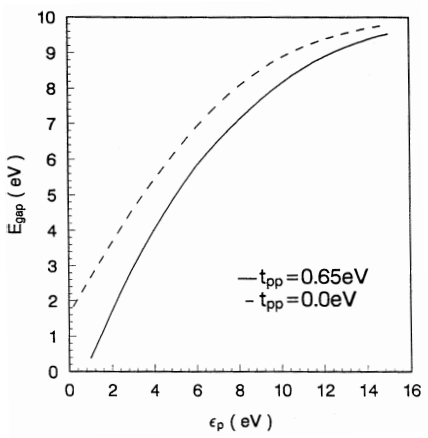

(a)

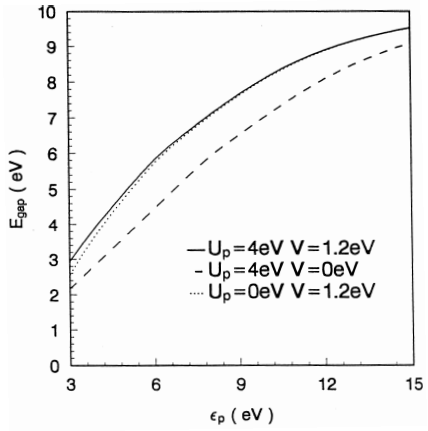

(b)

Fig. 6. Antiferromagnetic gap $E_{\rm gap}$ as a function of ε_p. (a) Solid line, $t_{pp} = 0.65$ eV; dashed line, $t_{pp} = 0$ eV. Other parameters: $t_{pd} = 1.3$ eV, $U_d = 10.5$ eV, $U_p = 4$ eV and $V = 1.2$ eV. (b) Curves for the variation of U_p and V. The solid line stands for $U_p = 4$ eV and $V = 1.2$ eV; the dashed line for $U_p = 4$ eV and $V = 0$ eV; the dotted line for $U_p = 0$ eV and $V = 1.2$ eV. The other parameters taken as (a).

considered, the gap has a finite value at $\varepsilon_p = 0$. As showed above, it can be seen here that the effect of t_{pp} and V on the results is larger than that of U_p. Taking $\varepsilon_p = 3.6$ eV, $t_{pp} = 0.65$ eV, we can obtain $E_{\rm gap} \approx 3.6$, which is very close to ε_p. So, a charge-transfer insulator is obtained and the charge-transfer gap that the mean field approach predicts nearly equals to the bare charge-transfer gap ε_p, but larger than its experimental value ≈ 2 eV.[27] This indicates that the description for the first excitation state of the holes in the mean field picture is not good. Following Zhang and Rice,[3] the spin singlet state is considered as the first excitation state

and then the charge-transfer gap is

$$\Delta_{\rm CT} = E_{\rm s} - 2E_{\rm AF}\,, \tag{16}$$

where $E_{\rm s}$ is the energy of the singlet state and $E_{\rm AF}$ is the energy of a hole in the AFM state as defined by Eq. (11). Equation (16) may be understood as energy enhancement of the system when a hole in the AFM state is taken from one place and added to another place and forms the singlet state with another hole, if the effect of this course on the AFM background is neglected. One can also understand Eq. (16) as the energy enhancement of the system when a hole added to the AFM background forms the singlet state with another hole in the AFM state. According to Ref. 3, we can estimate $E_{\rm s}$ as

$$E_{\rm s} = \tilde{\varepsilon}_p - 2\tilde{t}_{pd}\left(\frac{1}{\tilde{\varepsilon}_p + \tilde{U}_p} + \frac{1}{U_d - \tilde{\varepsilon}_p}\right)\,, \tag{17}$$

with

$$\tilde{\varepsilon}_p = \varepsilon_p - \mu_0 t_{pp} + f_0 + 4f_1 V\langle n_d\rangle\,,$$
$$\tilde{t}_{pd} = 2\lambda_0 t_{pd}\,,$$

and

$$\tilde{U}_p = h_0 U_p\,,$$

where $\mu_0 = 1.5$, $\lambda_0 = 0.96$, $f_0 = 0.92$, $h_0 = 0.29$, and $f_1 = 0.13$ were given by Belinicher and Chernyshev.[14] Using Eqs. (16) and (17) and taking the values of the parameters of the three-band model as above, we can obtain the charge-transfer gap $\Delta_{\rm CT} \approx 2.5$ eV. This value is in good agreement with the calculation result of Hybertsen *et al.*[12] and the experimental results.[26] Therefore, according to our calculation, the first excitation of hole indeed is the singlet state. This is in accordance with the recent experimental result in CuO[15] that the top of the valence band is of pure singlet character.

3.2. *Case of the doping*

Having discussed the case of the half-filling, let us now turn our attention to the hole-doping in the AFM background. According to the results at the half-filling, we expect that the doped holes should be added to the BUB band and the AFM state will be affected by the doping. We have carried out the calculation for the electronic structure and the magnetic properties via the mean field approximation. However, the effect of the doping on the AFM state turns out to be very small. In Fig. 7, we present the dependence of magnetic moment on the doping-density $\delta = n - 1$. We notice that the moment decreases with the increasing doping very slowly and the long-range AFM order persist till a large doping-density (~ 0.7). This result is not satisfying for the description of the realistic situation. In our mean field treatment, the uniform local magnetic moment is assumed. As mentioned by

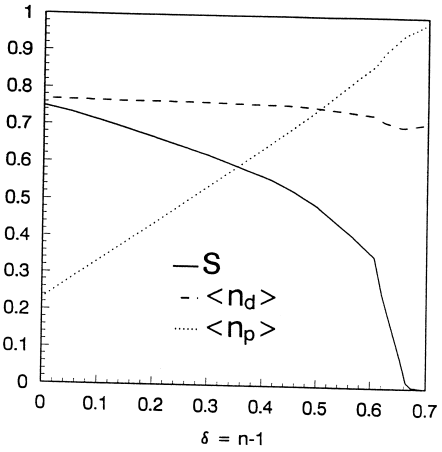

Fig. 7. Magnetic moment S (solid line), hole densities $\langle n_d \rangle$ (dashed line) and $\langle n_p \rangle$ (dotted line) as functions of doping-density $\delta = n - 1$. Parameters: $\varepsilon_p = 3.6$ eV, $t_{pd} = 1.3$ eV, $t_{pp} = 0.65$ eV, $U_d = 10.5$ eV, $U_p = 4$ eV and $V = 1.2$ eV.

Oles and Janzaanen,[20] this assumption is not correct. If a non-uniform distribution of magnetic moment S_i is considered, for instance, the orientation of the moment has some random distribution (or fluctuation), the results are expected to improve. Figure 7 also shows that the increase of p-hole is accompanied by rather small decrease of d-hole density with the increasing doping-density, so the new added holes are dominantly of oxygen character, as observed experimentally.[23] But the small decrease of d-hole is not in agreement with experiment. Therefore, in the uniform mean field picture, we can not give the correct description of hole-state under the doping. The true description of the doped holes has to be of the singlet state as mentioned above.

3.3. *Effective one-band Hubbard model*

It is important to reduce the three-band model to an one-band model in the study of the electronic properties of the cuprates. As is mentioned in Sec. 1, a great deal of effort has been made to present the effective one-band models. Here, based on our mean-field results, we present the following effective one-band Hubbard Hamiltonian,

$$H_{\text{eff}} = t_{\text{eff}} \sum_{\langle i,j \rangle,\sigma} c^{+}_{i\sigma} c_{j\sigma} + U_{\text{eff}} \sum_{i} c^{+}_{i\uparrow} c^{+}_{i\downarrow} c_{i\downarrow} c_{i\uparrow} \,. \tag{18}$$

Because the doping only connects with the BLH and BUH bands, at least in the case of underdoping, we can mimic the mean field charge-transfer gap E_{gap} by means of an effective Coulomb repulsion U_{eff} and reproduce the BLH (or BUH) band-width by an effective hopping t_{eff}. According to the AFM solution[25] of mean field for the one-band Hubbard model, we present the correspondence relation as

$$e_{\rm gap} = SU_{\rm eff}\,,$$
$$W = \sqrt{(4t_{\rm eff})^2 + (E_{\rm gap}/2)^2} - E_{\rm gap}/2\,, \tag{19}$$

where W is the BLH (or BUH) band-width and our calculation gives $S \approx 0.75$, $E_{\rm gap} \approx 3.6$ eV, $W_{\rm BLH} \approx 0.77$ eV and $W_{\rm BUH} \approx 1.0$ eV. And then, according to Eq. (18), we can obtain $U_{\rm eff} \approx 4.8$ eV and $t_{\rm eff} \approx 0.46$ eV for electron doping and $t_{\rm eff} \approx 0.54$ eV for hole doping. These values are close to the range of the parameters in the effective one-band Hubbard model presented by Hybertsen *et al.*[12]

4. Conclusion

Now, we conclude our results by summary. In the mean field picture, we have studied the electronic structure and the magnetic properties of CuO_2 planes of the cuprates, mainly for the half-filling, in the framework of the three-band model. We have considered the full three-band Hubbard Hamiltonian in which the direct O-O and Cu-O hopping and the repulsion on the copper and oxygen and between them are all taken into account. The extensively accepted values of the three-band model have been taken, which are $U_d = 10.5$ eV, $t_{pd} = 1.3$ eV, $t_{pp} = 0.65$ eV, $\varepsilon_p = 3.6$ eV, $U_p = 0.4$ eV and $V = 1.2$ eV (from Ref. 6).

First we presented the densities of states and the energy spectra for the insulating AFM ground state at the half-filling and show that only the two lowest bands — BLH and BUH bands are related to the doping. The superexchange interaction J, the composition of the holes and the magnetic moment S are calculated and the results are that $J \approx 0.12$ eV, the composition of the holes is Cu (77%) and O (23%) and $S \approx 0.75$. These values (except for the moment) are in agreement with the experiments[22,23] and calculations results[12] on clusters. Because the spin fluctuation is neglected in mean field approximation, the moment is larger, compared with experiment.[24,25] Meanwhile, the dependence of these electronic properties on the parameters of the model has also been discussed and we found that the influence of the O-O hopping (t_{pp}) and Cu-O intrasite Coulomb repulsion (V) on these results is remarkable, while the influence of repulsion on O sites is relatively small. For instance, the contribution from O-O hopping t_{pp} to J is about 2/3 of the total value, in accordance with the exact cluster calculations made by Eskes and Jefferson. Following Zhang and Rice,[3] we have calculated the energy of the spin singlet state above the AFM background and showed that the lowest excitation state of holes at the half-filling is the singlet state and then gave the charge-transfer gap of $\Delta_{\rm CT} \approx 2.5$ eV. Furthermore, we have also discussed the effect of the hole-doping on the AFM state and found that in the mean field picture the correct results can not be obtained. So, we conclude that the mean field approximation may give a good description of the ground state, but is not good for the doping case. Finally, according to the electronic structure we obtained at the half-filling, we present an effective one-band Hubbard model and the effective parameters of the model are

$U_{\text{eff}} \approx 4.8$ eV and $t_{\text{eff}} \approx 0.46$ eV for electron doping and $t_{\text{eff}} \approx 0.54$ eV for hole doping, close to the values given in Ref. 12.

References

1. P. W. Anderson, *Science* **235**, 1196 (1987).
2. V. Emery, *Phys. Rev. Lett.* **58**, 2794 (1987); J. Hirsch, *ibid.* **59**, 228 (1987); C. Varma *et al. Solid State Commun.* **62**, 681 (1987).
3. F. C. Zhang and T. M. Rice, *Phys. Rev.* **B37**, 3759 (1988).
4. S. Caprara and M. Grilli, *Phys. Rev.* **B49**, 6971 (1994).
5. F. Mancini, *Phys. Rev.* **B49**, 1350 (1994).
6. E. Dagotto, *Rev. Mod. Phys.* **66**, 763 (1994).
7. V. J. Emery and G. Reiter, *Phys. Rev.* **B38**, 11938 (1988).
8. F. C. Zhang and T. M. Rice, *Phys. Rev.* **B41**, 7243 (1990).
9. V. J. Emery and G. Reiter, *Phys. Rev.* **B41**, 7247 (1990).
10. C.-X. Chen, H. B. Schuttler and A. J. Fedro, *Phys. Rev.* **B41**, 2581 (1990).
11. H. B. Schutter and A. J. Fedro, *Phys. Rev.* **B45**, 7588 (1992).
12. M. S. Hybertsen, E. B. Stechel, M. Schluter and D. R. Jennison, *Phys. Rev.* **B41**, 11068 (1990).
13. H. Eskes and G. A. Sawatzky, *Phys. Rev. Lett.* **61**, 1415 (1988); F. Mila, *Phys. Rev.* **B38**, 11358 (1988); E. B. Stechel and D. R. Jennison, *ibid.* **B38**, 4632 (1988); J. Zaanen and A. M. Oles, *ibid.* **B37**, 9433 (1988); A. Ramasak and P. Prelovsek, *ibid.* **B40**, 2239 (1989); and V. I. Belinicher and A. L. Chernyshev, *ibid.* **B47**, 390 (1993).
14. V. I. Belinicher and A. L. Chernyshev, *Phys. Rev.* **B49**, 9746 (1994).
15. L. H. Tjeng *et al.*, *Phys. Rev. Lett.* **78**, 1126 (1997).
16. R. T. Scalettar, D. J. Scalapino, R. L. Sugar and S. R. White, *Phys. Rev.* **B44**, 770 (1991).
17. G. Dopf, A. Muramatsu and W. Hanke, *Phys. Rev.* **B41**, 9246 (1990).
18. J. E. Hirsch, S. Tange, E. Loh, Jr., D. J. Scalapino and S. Tang, *Phys. Rev.* **B39**, 243 (1989).
19. P. Unger and P. Fulde, *Phys. Rev.* **B47**, 8947 (1993).
20. A. M. Oles and J. Zaanen, *Phys. Rev.* **B39**, 9175 (1989).
21. H. Eskes and J. H. Jefferson, *Phys. Rev.* **B48**, 9788 (1993).
22. R. R. P. Singh, P. A. Fleury, K. B. Lyons and P. E. Sulewski, *Phys. Rev. Lett.* **62**, 2736 (1989); G. Aeppli *et al.*, *ibid.* **62**, 2052 (1988); Y. Endoh *et al.*, *Phys. Rev.* **B37**, 7443 (1988); K. Yamada *et al.*, *ibid.* **B40**, 4557 (1989).
23. J. D. Reger and A. P. Young, *Phys. Rev.* **B37**, 5978 (1988); D. Vankin *et al.*, *Phys. Rev. Lett.* **58**, 2802 (1987).
24. D. Vaknin, S. K. Sinha, D. E. Moneton, D. C. Johnston, J. M. Newsam, C. R. Safinya and H. E. King, Jr., *Phys. Rev. Lett.* **58**, 2802 (1987).
25. J. M. Tranquada, D. E. Cox, W. Kunnmann, H. Moundden, G. Shirane, S. K. Sinha, M. S. Alvarez, A. J. Jacobson, *Phys. Rev. Lett.* **60**, 156 (1988); W. H. Li, J. W. Lynn, H. A. Mook, B. S. Sales and Z. Fisk, *Phys. Rev.* **B37**, 9844 (1988); J. M. Tranquada *et al.*, *ibid.* **B38**, 2477 (1988).
26. J. R. Schrieffer, X. G. Wen and S. C. Zhang, *Phys. Rev.* **B39**, 11663 (1989).
27. J. M. Ginder, M. G. Ros, Y. Song, R. P. Macall, J. R. Gaines, E. Ehrenfreund and A. J. Epstein, *Phys. Rev.* **B37**, 7506 (1988); J. M. Humlicek and M. Cardona, *Solid State Commun.* **67**, 589 (1988).